3922 *Organometallics* **2010,** *29,* 3922–3929
DOI: 10.1021/om100579e

ORGANOMETALLICS
Article

2-Thia-1,3,5-triaza-7-phosphaadamantane-2,2-dioxide Revisited: Computational and Experimental Studies of a Neglected Phosphine

Michelle Sternberg,[†] Cherumuttathu H. Suresh,[‡] and Fabian Mohr*,[†]

[†]*Fachbereich C, Anorganische Chemie, Bergische Universität Wuppertal, 42119 Wuppertal, Germany, and* [‡]*Computational Modeling and Simulation Section, National Institute for Interdisciplinary Science and Technology (CSIR), Trivandrum 695 019, India*

Received June 12, 2010

The cage-phosphine 2-thia-1,3,5-triaza-7-phosphaadamantane-2,2-dioxide ($PASO_2$) was reacted with various transition metal precursors to give the complexes *cis*-$[Mo(CO)_4(PASO_2)_2]$, $[AuCl(PASO_2)]$, *cis*-$[PtCl_2(PASO_2)_2]$, $[Ru(\eta^6\text{-}p\text{-cym})Cl_2(PASO_2)]$, $[Rh(\eta^5\text{-}C_5Me_5)Cl_2(PASO_2)]$, and $[Rh(\eta^5\text{-}C_5Me_5)Cl(PASO_2)_2]^+$ as well as the cyclometalated palladium(II) complexes $[PdCl\{\kappa C,N\text{-}C_6H_4C(Ph)NCH_2CO_2Et\}(PASO_2)]$ and $[PdCl(\kappa C,N\text{-}1,8\text{-}C_{10}H_6NMe_2)(PASO_2)]$. The compounds were characterized by spectroscopic methods and several examples by single-crystal X-ray diffraction. The stereoelectronic properties of $PASO_2$ were determined by computational methods and were compared with those of other phosphines, in particular 1,3,5-triaza-7-phosphaadamantane.

Introduction

Development of the coordination chemistry of the sterically small, water-soluble cage phosphine 1,3,5-triaza-7-phosphaadamantane (abbreviated in the literature as both PTA and TPA) has seen rapid growth in the past 15 years,[1,2] although the compound itself has been known since 1974.[3,4] More recently, a variety of modified analogues of PTA and their metal complexes have been reported including N-alkylated compounds,[5−8] open-cage derivatives,[7,9,10] "upper-rim"-functionalized derivatives derived from the lithium salt,[11] and "lower-rim" analogues,[12] shown in Chart 1.

One analogue of PTA, 2-thia-1,3,5-triaza-7-phosphaadamantane-2,2-dioxide ($PASO_2$), in which one NCH_2N methylene bridge is replaced by an SO_2 group, has been almost entirely neglected. The compound was first reported by Daigle in 1974,[3] and its crystal structure was published two years later.[13] Since then, only one paper describing the tungsten carbonyl complex, $[W(CO)_5(PASO_2)]$, as well as some reactivity studies has appeared.[14] Although $PASO_2$ is not soluble in water, its coordination chemistry nevertheless warrants more exploration. Given our interest in precious metal complexes containing PTA and their applications,[15−20] we report here an extended chemical and computational study of the coordination chemistry of $PASO_2$.

Results and Discussion

In order to get a better understanding of the electronic properties of $PASO_2$, we initially prepared the molybdenum carbonyl complex *cis*-$[Mo(CO)_4(PASO_2)_2]$ (**1**), which was readily accessible from the reaction of *cis*-$[Mo(CO)_4(pip)_2]$ (pip = piperidine) with two equivalents of $PASO_2$, and examined its IR spectrum. The solid-state IR spectrum of **1** reveals four bands for the CO stretching frequencies, as expected for a C_{2v}-symmetric *cis*-$[M(CO)_4L_2]$-type complex. For comparison, we also measured the solid-state IR spectrum of the PTA analogue, since in the literature only

*To whom correspondence should be addressed. E-mail: fmohr@uni-wuppertal.de.

(1) Phillips, A. D.; Gonsalvi, L.; Romerosa, A.; Vizza, F.; Peruzzini, M. *Coord. Chem. Rev.* **2004**, *248*, 955.
(2) Bravo, J.; Bolano, S.; Gonsalvi, L.; Peruzzini, M. *Coord. Chem. Rev.* **2010**, *254*, 555.
(3) Daigle, D. J.; Pepperman, A. B., Jr.; Vail, S. L. *J. Heterocycl. Chem.* **1974**, *11*, 407.
(4) Fluck, E.; Förster, J. E. *Chem. Zeitung* **1975**, *99*, 246.
(5) Daigle, D. J.; Pepperman, A. B., Jr. *J. Heterocycl. Chem.* **1975**, *12*, 579.
(6) Pruchnik, F. P.; Smolenski, P.; Galdecka, E.; Galdecki, Z. S. *Inorg. Chim. Acta* **1999**, *293*, 110.
(7) Krogstad, D. A.; Ellis, G. S.; Gunderson, A. K.; Hammrich, A. J.; Rudolf, J. W.; Halfen, J. A. *Polyhedron* **2007**, *26*, 4093.
(8) Krogstad, D. A.; Gohmann, K. E.; Sunderland, T. L.; Geis, A. L.; Bergamini, P.; Marvelli, L.; Young, V. G. *Inorg. Chim. Acta* **2009**, *362*, 3049.
(9) Darensbourg, D. J.; Ortiz, C. G.; Kamplain, J. W. *Organometallics* **2004**, *23*, 1747.
(10) Mena-Cruz, A.; Lorenzo-Luis, P.; Romerosa, A.; Saoud, M.; Serrano-Ruiz, M. *Inorg. Chem.* **2007**, *46*, 6120.
(11) Wong, G. W.; Harkreader, J. L.; Mebi, C. A.; Frost, B. J. *Inorg. Chem.* **2006**, *45*, 6748.
(12) Huang, R.; Frost, B. J. *Inorg. Chem.* **2007**, *46*, 10962.
(13) Delerno, J. R.; Majeste, R. J.; Trefonas, L. M. *J. Heterocycl. Chem.* **1976**, *13*, 757.
(14) Darensbourg, D. J.; Yarbrough, J. C.; Lewis, S. J. *Organometallics* **2003**, *22*, 2050.
(15) *Gold Chemistry. Applications and Future Directions in the Life Sciences*; Mohr, F., Ed.; Wiley-VCH: Weinheim, 2009.
(16) Mohr, F.; Cerrada, E.; Laguna, M. *Organometallics* **2006**, *25*, 644.
(17) Mohr, F.; Sanz, S.; Tiekink, E. R. T.; Laguna, M. *Organometallics* **2006**, *25*, 3084.
(18) Vergara, E.; Miranda, S.; Mohr, F.; Cerrada, E.; Tiekink, E. R. T.; Romero, P.; Laguna, M. *Eur. J. Inorg. Chem.* **2007**, 2926.
(19) Miranda, S.; Vergara, E.; Mohr, F.; de Vos, D.; Cerrada, E.; Mendía, A.; Laguna, M. *Inorg. Chem.* **2008**, *47*, 5641.
(20) Dolfen, D.; Schottler, K.; Seied-Mojtaba, V.; Jakupec, M. A.; Keppler, B. K.; Tiekink, E. R. T.; Mohr, F. *J. Inorg. Biochem.* **2008**, *102*, 2067.

 Published on Web 08/12/2010

Chart 1

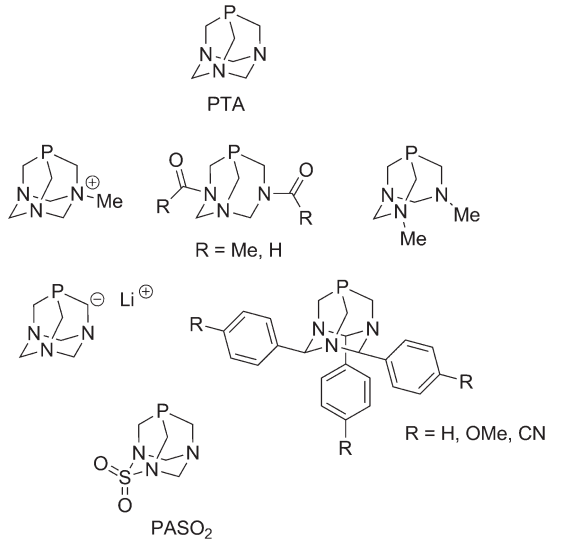

solution IR data were available.[21] The results show that, in particular, the positions of the A1 band at 2033 cm^{-1} ($PASO_2$) and 2014 cm^{-1} (PTA) are significantly different in the two complexes, indicating that despite their apparent structural similarity, the electronic properties of PTA and $PASO_2$ are quite different. This observation is in marked contrast to the previous paper comparing IR data of the W-complexes $[W(CO)_5L]$ (L = PTA, $PASO_2$), in which no significant CO band shifts were observed, leading the authors to conclude that the two phosphines are quite similar in electronic character.[14] On the basis of our experimental data we can qualitatively conclude that $PASO_2$ is a stronger π-acid (π-acceptor) than PTA.

To confirm this finding, we carried out a computational study on the two phosphines using the total electronic (E_{eff}) and steric effects (S_{eff}) methodology developed by Suresh and co-workers.[22] The results are shown in Table 2, where the V_{min} values correspond to the molecular electrostatic potential minimum at the lone pair region of the phosphorus.[23,24] The $V_{min}(PASO_2)$ is determined using the B3LYP/6-31G(d,p) method, while $V_{min}(ONIOM\_PASO_2)$ is calculated using the ONIOM(B3LYP/6-31G(d,p):UFF) hybrid QM-MM method.[25,26] The computational data indeed

Table 1. Summary of the Computed Steroelectronic Properties of $PASO_2$ and PTA

	$V_{min}(PR_3)$, kcal/mol	$S_{eff}+E_{eff}$, kcal/mol	$V_{min}(ONIOM\_PR_3)$, kcal/mol	S_{eff}, kcal/mol	E_{eff}, kcal/mol
$PASO_2$	−20.68	−7.54	−36.36	8.14	−15.68
PTA	−33.69	5.48	−30.62	3.07	2.40

Table 2. Comparison of ^{31}P NMR Data for $PASO_2$ and PTA Complexes

compound	^{31}P chemical shift (recorded in dmso-d_6)	ΔP^a
$PASO_2$	−116.9	0.0
PTA	−104.1	0.0
$[AuCl(PASO_2)]$	−56.6	60.3
[AuCl(PTA)]	−52.1	52.0
cis-$[PtCl_2(PASO_2)_2]$	−64.0 (J_{P-Pt} = 3387 Hz)	52.9
cis-$[PtCl_2(PTA)_2]$	−53.0 (J_{P-Pt} = 3309 Hz)	51.1
cis-$[Pt(N_3)_2(PASO_2)_2]$	−68.9 (J_{P-Pt} = 3257 Hz)	48.0
cis-$[Pt(N_3)_2(PTA)_2]$[28]	−59.1 (J_{P-Pt} = 3140 Hz)	45.0

[a] ΔP is defined here as the chemical shift difference between the free phosphine and the coordinated phosphine.

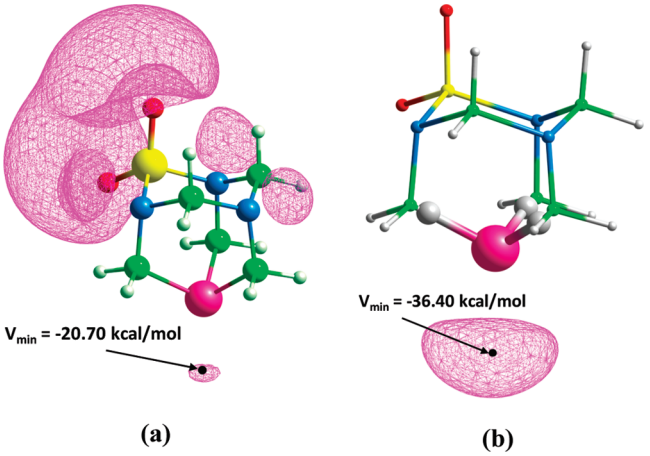

Figure 1. Molecular electrostatic potential isosurface map of value −18.83 kcal/mol for the PASO2 ligand. (a) B3LYP/6-31G(d,p) result. (b) ONIOM(B3LYP/6-31G(d,p):UFF) result. In (b), the stick representation is used to show the UFF region, which is linked to the QM region via H atoms. The value of V_{min} is also indicated with a black dot.

confirm the significantly different stereoelectronic properties of the two phosphines. The data show that $PASO_2$ combines a high electron-donating steric effect with a high withdrawing electronic effect. This high electron-withdrawing nature originates from the SO_2 unit, which can clearly been seen from the molecular electrostatic potential isosurface map given in Figure 1. PTA, in contrast, shows a much weaker electron-donating steric effect and is weakly electron donating, as can be seen from the plot in Figure 2, where the stereoelectronic profile of typical phosphine ligands and two phosphate ligands are also depicted for comparison.[22] The electron-withdrawing power of the $PASO_2$ ligand (E_{eff} = −15.68 kcal/mol) is comparable to that of phosphate ligands QIVLOW (E_{eff} = −15.20 kcal/mol) and HAZXOV (E_{eff} = −12.92 kcal/mol), whereas its electron-donating steric effect (S_{eff} = 8.14 kcal/mol) is significantly higher than these ligands (S_{eff} is 3.30 kcal/mol QIVLOW and −3.12 kcal/mol for HAZXOV).[22] The steric effect of $PASO_2$ is as strong as the relatively bulky $P(^iPr)_3$ ligand.

(21) Darensbourg, D. J.; Kump, R. L. *Inorg. Chem.* **1978**, *17*, 2680.
(22) Mathew, J.; Thomas, T.; Suresh, C. H. *Inorg. Chem.* **2007**, *47*, 10800.
(23) Suresh, C. H. *Inorg. Chem.* **2006**, *45*, 4982.
(24) Suresh, C. H.; Koga, N. *Inorg. Chem.* **2002**, *41*, 1573.
(25) Vreven, T.; Morokuma, K. *J. Comput. Chem.* **2000**, *21*, 1419.
(26) Frisch, M. J.; Trucks, G. W.; Schlegel, H. B.; Scuseria, G. E.; Robb, M. A.; Cheeseman, J. R.; Montgomery, J. A.; Vreven, T.; Kudin, K. N.; Burant, J. C.; Millam, J. M.; Yengar, S. S.; Tomasi, J.; Barone, V.; Mennucci, B.; Cossi, M.; Scalmani, G.; Rega, N.; Petersson, G. A.; Nakatsuji, H.; Hada, M.; Ehara, M.; Toyota, K.; Fukuda, R.; Hasegawa, J.; Ishida, M.; Nakajima, T.; Honda, Y.; Kitao, O.; Nakai, H.; Klene, M.; Li, X.; Knox, J. E.; Hratchian, H. P.; Cross, J. B.; Bakken, V.; Adamo, C.; Jaramillo, J.; Gomperts, R.; Stratmann, R. E.; Yazyev, O.; Austin, A. J.; Cammi, R.; Pomelli, C.; Ochterski, J. W.; Ayala, P. Y.; Morokuma, K.; Voth, G. A.; Salvador, P.; Dannenberg, J. J.; Zakrzewski, V. G.; Dapprich, S.; Daniels, A. D.; Strain, M. C.; Farkas, O.; Malick, D. K.; Rabuck, A. D.; Raghavachari, K.; Foresman, J. B.; Ortiz, J. V.; Cui, Q.; Baboul, A. G.; Clifford, S.; Cioslowski, J.; Stefanov, B. B.; Liu, G.; Liashenko, A.; Piskorz, P.; Komaromi, I.; Martin, R. L.; Fox, D. J.; Keith, T.; Al-Laham, M. A.; Peng, C. Y.; Nanayakkara, A.; Challacombe, M.; Gill, P. M. W.; Johnson, B.; Chen, W.; Wong, M. W.; Gonzalez, C.; Pople, J. A. *Gaussian 03*, Revision E.01; Gaussian, Inc., 2004.

Scheme 1

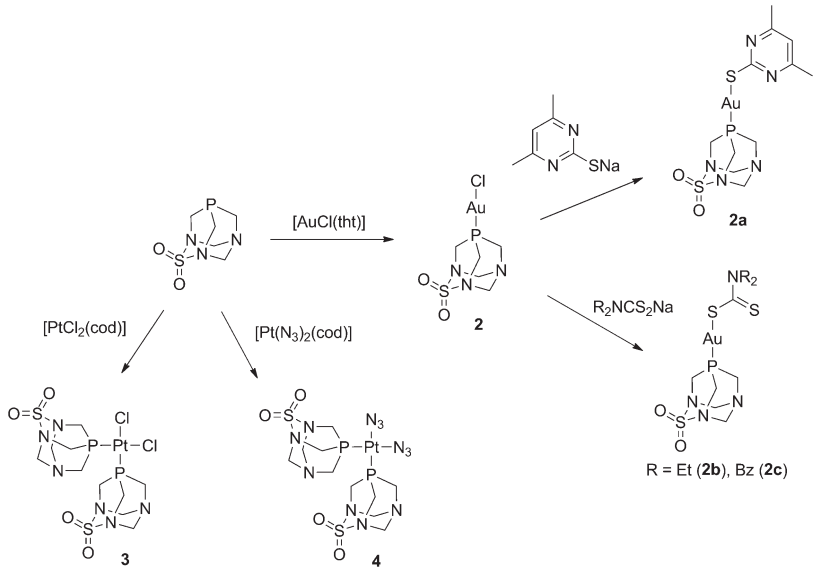

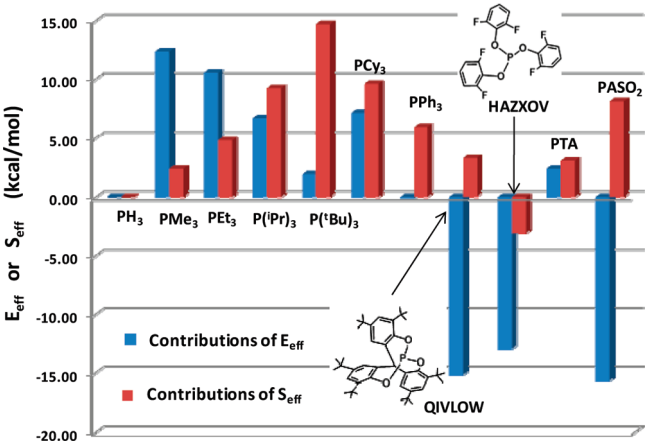

Figure 2. Stereoelectronic plot of phosphine ligands. Data (except those for $PASO_2$) are taken from ref 22.

Gold(I) and Platinum(II) Complexes. $PASO_2$ readily displaces the weakly coordinating ligands in [AuCl(tht)] (tht = tetrahydrothiophene) and *cis*-[$PtCl_2$(cod)] (cod = 1,5-cyclooctadiene) to give [AuCl($PASO_2$)] (**2**) and *cis*-[$PtCl_2$($PASO_2$)$_2$] (**3**), respectively, in high yields. Both complexes are insoluble in water and poorly soluble in most solvents including dmso and dmf. In an attempt to improve solubility, we prepared several derivatives by anion exchange of the chloride ligands. The thiolato gold(I) complexes [Au(SR)($PASO_2$)] (R = 3,5-dimethylpyrimidyl, **2a**) and [Au(S_2CNR_2)($PASO_2$)] (R = Et, **2b**; Bz, **2c**) were prepared by treatment of **2** with the sodium salt of 3,5-dimethylpyrimidinethiol or sodium diethyl- and dibenzyldithiocarbamate (Scheme 1). In addition, the azido Pt complex *cis*-[$Pt(N_3)_2$($PASO_2$)$_2$] (**4**) was prepared by displacement of cod from *cis*-[$Pt(N_2)_3$(cod)] by $PASO_2$, as shown in Scheme 1. We also tried to prepare gold(I) alkynyl complexes by the reaction of **2** with alkynes in the presence of base. However, due to the poor solubility of **2**, only starting materials were recovered even after prolonged reaction times.

Complexes **2**−**4** are also insoluble in common solvents including water, acetone, acetonitrile, alcohols, and halogenated solvents and dissolve only poorly in dmso and dmf. Thus, exchange of the chloride ligands with other ligands containing aliphatic and aromatic substituents does not lead to an improved solubility in organic solvents.

The compounds were however soluble enough in dmso to allow characterization by NMR spectroscopy. The ^{1}H NMR spectra of compounds **2**−**4** show, in addition to other ligand signals, two AB quartets and one singlet resonance for the $PASO_2$ protons. The singlet is due to the PCH_2N group that lies in the plane bisecting the SO_2 unit, while the AB system arises from inequivalent axial and equatorial methylene group protons. Similarly to what has been observed in many metal complexes containing PTA, the PCH_2N protons in $PASO_2$ metal complexes do not display coupling with the phosphorus atom. We could unambiguously assign the PCH_2N and NCH_2N protons by using ^{13}C−^{1}H 2D NMR spectroscopy (see Experimental Section for details). The ^{31}P NMR spectra of complexes **2**−**4** show singlet resonances at around −60 ppm, which are shifted by ca. 60 ppm from the resonance of free $PASO_2$ (−116.9 ppm). In the case of the Pt complexes **3** and **4**, Pt satellites with coupling constants of ca. 3300 Hz are also observed. The magnitude of these Pt−P coupling constants is consistent with a *cis* geometry about the platinum atom. This has been confirmed by an X-ray structure of the PTA derivative *cis*-[$Pt(N_3)_2$($PTA)_2$], which shows a very similar Pt−P coupling constant of 3140 Hz in its ^{31}P NMR spectrum.[27]

Since both ^{31}P chemical shifts as well as the magnitude of the Pt−P coupling constants in metal phosphine complexes are affected by the nature of the phosphine, it is appropriate to compare the data of some $PASO_2$ and PTA complexes (Table 2).

It can be seen that the ^{31}P NMR chemical shifts of the Au and Pt $PASO_2$ complexes experience a higher coordination shift (ΔP) than those of the analogous PTA complexes. In addition, the Pt−P coupling constant is considerably larger in the $PASO_2$ derivatives. The downfield shift is due to removal of electron density at phosphorus (due to coordination to the metal). These data show that despite their structural similarity,

(27) Smoleski, P.; Mukhopadhyay, S.; Guedes da Silva, M. F. C.; Adília Januário Charmier, M.; Pombeiro, A. J. L. *Dalton Trans.* **2008**, 6546.
(28) Fleischer, A.; Roller, A.; Arion, V. B.; Keppler, B. K.; Mohr, F. *Can. J. Chem.* **2009**, *87*, 146.

Scheme 2

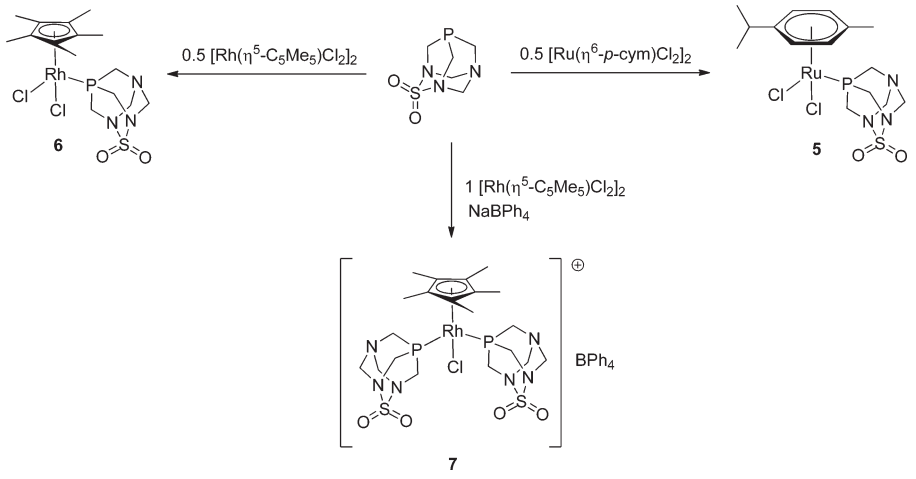

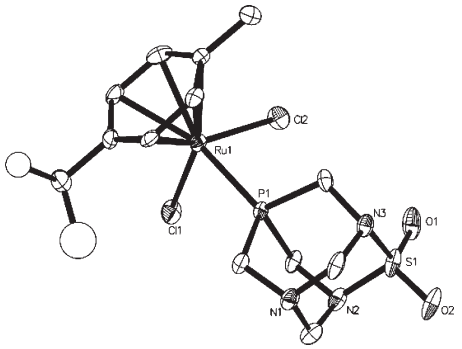

Figure 3. Molecular structure of compound **5**. Ellipsoids show 50% probability levels. Hydrogen atoms have been omitted for clarity.

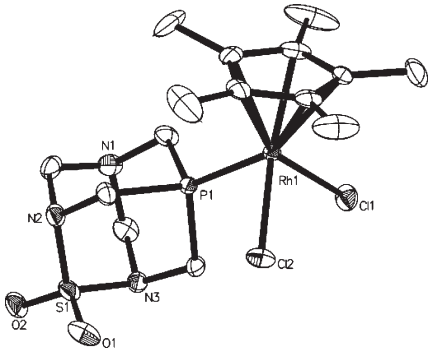

Figure 4. Molecular structure of compound **6**. Ellipsoids show 50% probability levels. Hydrogen atoms have been omitted for clarity.

$PASO_2$ has a different influence on the ^{31}P NMR chemical shift and the Pt−P coupling constants than PTA.

Organometallic Ruthenium(II) and Rhodium(III) Complexes. Two equivalents of $PASO_2$ react with the Ru(II) and Rh(III) dimers $[Ru(\eta^6\text{-}p\text{-cym})Cl_2]_2$ and $[Rh(\eta^5\text{-}C_5Me_5)Cl_2]_2$ to give the monomeric Ru and Rh complexes $[Ru(\eta^6\text{-}p\text{-cym})Cl_2(PASO_2)]$ (**5**) and $[Rh(\eta^5\text{-}C_5Me_5)Cl_2(PASO_2)]$ (**6**), respectively (Scheme 2). Similarly, the reaction of $[Rh(\eta^5\text{-}C_5Me_5)Cl_2]_2$ with four equivalents of $PASO_2$ affords the cationic Rh(III) complex $[Rh(\eta^5\text{-}C_5Me_5)Cl(PASO_2)_2]^+$, which was isolated as the BPh_4 salt (**7**).

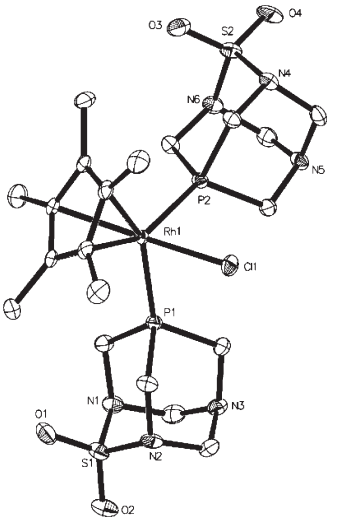

Figure 5. Molecular structure of one of the independent molecules of compound **7a**. Ellipsoids show 50% probability levels. Hydrogen atoms as well as the Cl^- anion and the H_2O of crystallization have been omitted for clarity.

Table 3. Comparison of Selected Bond Distances in $PASO_2$ and PTA Ru and Rh Complexes

complex	M−P	M−Cl	M−C[a]
$[Ru(\eta^6\text{-}p\text{-cym})Cl_2(PASO_2)]$ (**5**)	2.2910(10)	2.4175(10) 2.4144(10)	1.699
$[Ru(\eta^6\text{-}p\text{-cym})Cl_2(PTA)]$[29]	2.296(2)[b] 2.298(3)	2.42[c] 2.43	1.692
$[Rh(\eta^5\text{-}C_5Me_5)Cl_2(PASO_2)]$ (**6**)	2.2657(6)	2.4115(5) 2.4117(6)	1.816
$[Rh(\eta^5\text{-}C_5Me_5)Cl_2(PTA)]$[30]	2.286(1)	2.410(1) 2.417(1)	1.804
$[Rh(\eta^5\text{-}C_5Me_5)Cl(PASO_2)_2]Cl$ (**7a**)	2.2957(7) 2.2942(6)	2.4010(6)	1.857
$[Rh(\eta^5\text{-}C_5Me_5)Cl(PTA)_2]Cl$[30]	2.291(2) 2.288(2)	2.405(2)	1.859

[a] Distance between the metal and the calculated centroid of the aromatic ring. [b] Two independent molecules per asymmetric unit. [c] Average distances from two independent molecules.

(29) Allardyce, C. S.; Dyson, P. J.; Ellis, D. J.; Heath, S. L. *Chem. Commun.* **2001**, 1396.
(30) Dorcier, A.; Ang, W. H.; Bolaño, S.; Gonsalvi, L.; Juillerat-Jeannerat, L.; Laurenczy, G.; Peruzzini, M.; Phillips, A. D.; Zanobini, F.; Dyson, P. J. *Organometallics* **2006**, *25*, 4090.

Scheme 3

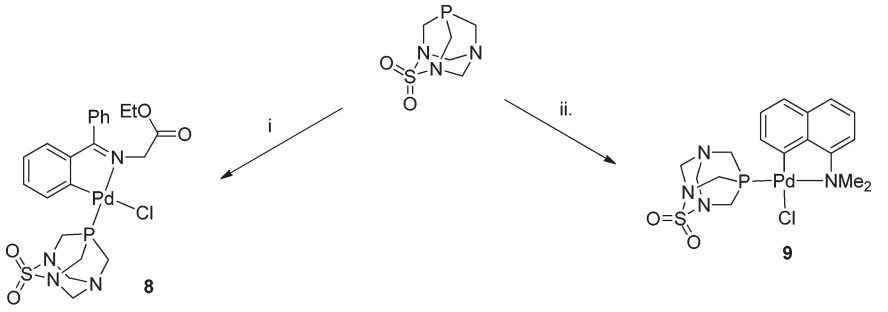

i: 0.5 $[PdCl\{C_6H_4C(Ph)NCH_2CO_2Et\}]_2$; ii: 0.5 $[PdCl\{1,8\text{-}C_{10}H_6NMe_2\}]_2$

X-ray quality crystals of the chloride salt (**7a**) were obtained when a CH_2Cl_2 solution of $[Rh(\eta^5\text{-}C_5Me_5)Cl_2]_2$ containing an excess of $PASO_2$ was shaken with water in an attempt to extract the salt into the aqueous phase.

Complexes **5**−**7** are considerably more soluble than the aforementioned Au and Pt complexes. Although neither of them is soluble in water, they are soluble in acetone, acetonitrile, CH_2Cl_2, and dmso. This reasonable solubility in a wide range of solvents allowed us to obtain X-ray quality crystals of complexes **5**, **6**, and **7a**, the molecular structures of which are shown in Figures 3−5; selected bond distances together with those of the analogous PTA complexes are shown in Table 3.

The overall geometry of the half-sandwich "piano-stool" $PASO_2$ complexes **5**−**7a** is basically identical to that of the corresponding PTA[29,30] complexes and also typical for arene Ru(II) or Cp* Rh(III) phosphine complexes. While the M−P, M−Cl, and M−C_{ring} bond lengths of the Ru complex **5** and the cationic Rh complex **7a** are very similar for both $PASO_2$ and PTA, the neutral Cp* Rh $PASO_2$ complex **6** has a slightly shorter Rh−P bond distance but a longer Rh−C_{ring} bond distance when compared to those of its PTA analogue. These data show that the different stereoelectronic properties of the phosphines are not reflected in the structures (bond distances) of the complexes. How reactivity of the compounds, e.g., in catalysis, is influenced by the different phosphines is currently being investigated.

The NMR spectroscopic data of complexes **5**−**7** are similar to those of the Au and Pt complexes discussed above: singlet or doublet (P−Rh coupling) resonances for the Ru and Rh complexes, respectively, are observed in the ^{31}P NMR spectra. Unfortunately, there are no chemical shift data available in the same solvent for the PTA congeners, making a meaningful comparison difficult.

Cyclometalated Palladium(II) Complexes. $PASO_2$ reacts with the cyclometalated chloro-bridged Pd(II) dimers $[PdCl\{\kappa C,N\text{-}C_6H_4C(Ph)NCH_2CO_2Et\}]_2$ and $[PdCl\{\kappa C,N\text{-}1,8\text{-}C_{10}H_6NMe_2\}]_2$ to give the bridge cleavage products $[PdCl\{\kappa C,N\text{-}C_6H_4C(Ph)NCH_2CO_2Et\}(PASO_2)]$ (**8**) and $[PdCl(\kappa C,N\text{-}1,8\text{-}C_{10}H_6NMe_2)(PASO_2)]$ (**9**), respectively, as yellow solids in high yield (Scheme 3). Compounds **8** and **9** are insoluble in water, ether, and hexane but soluble in acetone and halogenated solvents. Single crystals were obtained of both compounds, which allowed us to determine the solid-state structure by X-ray diffraction. The molecular structures are shown in Figures 6 and 7.

In both compounds, the phosphine ligand is located *trans* to the nitrogen atom in the square-planar coordination environment about the palladium atom. This behavior is typically observed in bridge-cleavage reactions of chloro-bridged palladacycles with monodentate phosphines and is also consistent with the *transphobia* principle that explains the avoidance of mutually *trans* phosphorus and aryl carbon atoms at a palladium(II) center.[31] The bond distances and angles of complexes **8** and **9** are typical for orthometalated Pd phosphine complexes and are similar to those observed in the PTA complex $[PdCl\{\kappa C,N\text{-}C_6H_4CH_2NMe_2\}(PTA)]$, one of the very few known palladacycles containing PTA.[32,33]

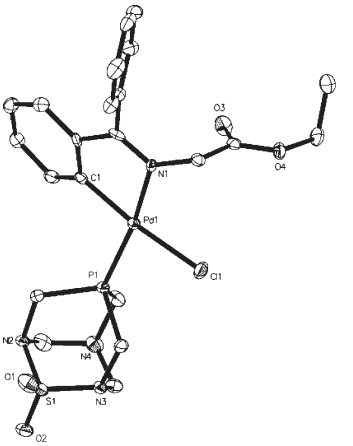

Figure 6. Molecular structure of compound **8**. Ellipsoids show 50% probability levels. Hydrogen atoms have been omitted for clarity.

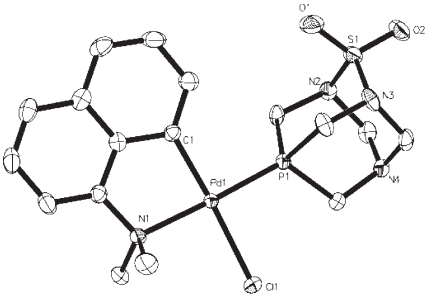

Figure 7. Molecular structure of compound **9**. Ellipsoids show 50% probability levels. Hydrogen atoms as well as the disordered CH_2Cl_2 molecule of solvation have been omitted for clarity.

(31) *Palladacycles*; Dupont, J.; Pfeffer, M., Eds.; Wiley-VCH: Weinheim, 2008.

(32) Ruiz, J.; Cutillas, N.; Lopez, F.; Lopez, G.; Bautista, D. *Organometallics* **2006**, *25*, 5768.

(33) Spencer, J.; Casini, A.; Zava, O.; Rathnam, R. P.; Velhanda, S. K.; Pfeffer, M.; Callear, S. K.; Hursthouse, M. B.; Dyson, P. J. *Dalton Trans.* **2009**, 10731.

In conclusion, we have shown by both computational and spectroscopic methods that $PASO_2$ is a phosphine with unique stereoelectronic properties. In terms of its chemical reactivity, the compound undergoes typical reactions of a phosphine with various transition metal precursors, which we demonstrated by examining its complexes containing Mo, Au, Pt, Pd, Ru, and Rh. Just how the stereoelectronic properties of $PASO_2$ influence the catalytic and biological properties of its complexes is currently being further investigated in our group.

Experimental Section

General Procedures. ^{1}H, ^{13}C, and ^{31}P{^{1}H} NMR spectra were recorded on a 400 MHz Bruker Avance spectrometer. Chemical shifts are quoted relative to external $SiMe_4$ (^{1}H, ^{13}C) and H_3PO_4 (^{31}P). Elemental analyses were performed by staff of the microanalytical laboratory of the University of Wuppertal. High-resolution electrospray mass spectra were recorded on a Bruker Daltonics MicroTOF instrument in positive ion mode from MeCN solutions. IR spectra were recorded on a Bruker Tensor 27 FT-IR spectrometer fitted with an ATR unit. All reactions were carried out under aerobic conditions unless stated otherwise. The phosphine $PASO_2$ as well as the metal precursors [AuCl(tht)] (tht = tetrahydrothiophene), *cis*-[$PtCl_2$(cod)], *cis*-[$Pt(N_3)_2$(cod)] (cod = 1,5-cyclooctadiene), [$Ru(\eta^6$-*p*-cym)$Cl_2]_2$ (*p*-cym = *p*-cymene), [$Rh(\eta^5$-$C_5Me_5)Cl_2]_2$, [PdCl{κC,*N*-C_6H_4C(Ph)NCH_2CO_2Et}]$_2$, [PdCl{κC,*N*-1,8-$C_{10}H_6NMe_2$}]$_2$, and *cis*-[$Mo(CO)_4$(pip)$_2$] (pip = piperidine) were prepared as described in the literature.[3,21,34−40] All other chemicals and solvents (HPLC or extra dry grade) were sourced commercially and used as received.

***cis*-[Mo(CO)$_4$(PASO$_2$)$_2$] (1).** A mixture of *cis*-[$Mo(CO)_4$(pip)$_2$] (0.150 g, 0.393 mmol) and $PASO_2$ (0.166 g, 0.801 mmol) in CH_2Cl_2 (15 mL) was heated under nitrogen to reflux for ca. 10 min. The resulting orange solution was passed through Celite and the filtrate concentrated under vacuum. Addition of MeOH precipitated the product as a pale yellow solid in 85% yield (0.208 g). ^{31}P{^{1}H} NMR (162 MHz, dmso-d_6): δ −61.4. ^{1}H NMR (400 MHz, dmso-d_6): δ 4.11 (s, 4 H, PCH_2NS), 4.62 (AB quart., J = 16.2 Hz, 8 H, PCH_2N), 5.01 (AB quart., J = 13.4 Hz, 8 H, NCH_2N). IR (ATR): 2033, 1923, 1872, 1825 ν(CO) cm^{-1}. Anal. Calcd for $C_{14}H_{24}N_6O_8P_2SMo$: C, 26.84; H, 3.86; N, 13.42. Found: C, 26.93; H, 3.77; N, 13.32.

[AuCl(PASO$_2$)] (2). To a solution of [AuCl(tht)] (0.100 g, 0.312 mmol) in CH_2Cl_2 (10 mL) was added a solution of $PASO_2$ (0.065 g, 0.314 mmol) in CH_2Cl_2 (15 mL). After ca. 30 min the colorless precipitate was isolated by filtration, washed with Et_2O, and dried in air. Yield: 0.124 g (91%). ^{31}P{^{1}H} NMR (162 MHz, dmso-d_6): δ −56.6. ^{1}H NMR (400 MHz, dmso-d_6): δ 4.35 (s, 2 H, PCH_2NS), 4.90 (AB quart., J = 15.6 Hz, 4 H, PCH_2N), 4.96 (AB quart., J = 13.2 Hz, 4 H, NCH_2N). Anal. Calcd for $C_5H_{10}N_3O_2PSClAu$: C, 13.66; H, 2.29; N, 9.56. Found: C, 13.55; H, 2.08; N, 9.23.

[Au(SMe$_2$pyrim)(PASO$_2$)] (2a). To a suspension of [AuCl($PASO_2$)] (0.044 g, 0.100 mmol) in MeOH (10 mL) was added the sodium salt of 3,5-dimethylpyrimidinethiol (0.017 g, 0.105 mmol). The mixture was left to stir for ca. 18 h. The precipitated colorless solid was isolated by filtration, washed with H_2O, MeOH, and Et_2O, and subsequently left to dry in air. Yield: 0.028 g (52%). ^{31}P{^{1}H} NMR (162 MHz, dmso-d_6): δ −53.6. ^{1}H NMR (400 MHz, dmso-d_6): δ 2.23 (s, 6 H, Me), 4.36 (s, 2 H, PCH_2NS), 4.69−5.20 (m, 8 H, PCH_2N, NCH_2N), 6.73 (s, 1 H, Arom). Anal. Calcd for $C_{11}H_{17}N_5O_2PS_2Au$: C, 24.32; H, 3.15; N, 12.89. Found: C, 24.11; H, 3.00; N, 13.16.

[Au(S$_2$CNEt$_2$)(PASO$_2$)] (2b). To a suspension of [AuCl($PASO_2$)] (0.100 g, 0.227 mmol) in MeOH (10 mL) was added the sodium diethyldithiocarbamate (0.056 g, 0.327 mmol). The mixture was left to stir for ca. 18 h. The precipitated dark yellow solid was isolated by filtration, washed with H_2O, MeOH, and Et_2O, and subsequently left to dry in air. Yield: 0.126 g (quantitative). ^{31}P{^{1}H} NMR (162 MHz, dmso-d_6): δ −60.9. ^{1}H NMR (400 MHz, dmso-d_6): δ 1.20 (t, J = 7.2 Hz, 6 H, Me), 3.78 (q, J = 7.2 Hz, 4 H, NCH_2), 4.28 (s, 2 H, PCH_2NS), 4.68−5.28 (m, 8 H, PCH_2N, NCH_2N). Anal. Calcd for $C_{10}H_{20}N_4O_2PS_3Au$: C, 21.74; H, 3.65; N, 10.14. Found: C, 21.66; H, 3.77; N, 10.40.

[Au(S$_2$CNBz$_2$)(PASO$_2$)] (2c). This was prepared as above from [AuCl($PASO_2$)] (0.100 g, 0.227 mmol) and sodium dibenzyldithiocarbamate (0.074 g, 0.251 mmol). Yield: 0.119 g (77%), pale yellow solid. ^{31}P{^{1}H} NMR (162 MHz, dmso-d_6): δ −58.7. ^{1}H NMR (400 MHz, dmso-d_6): δ 4.33 (s, 2 H, PCH_2NS), 4.73−5.25 (m, 10 H, PCH_2N, NCH_2N, NCH_2), 7.28−7.42 (m, 10 H, Ph). Anal. Calcd for $C_{20}H_{24}N_4O_2PS_3Au$: C, 35.50; H, 3.58; N, 8.28. Found: C, 35.83; H, 3.40; N, 8.51.

***cis*-[PtCl$_2$(PASO$_2$)$_2$] (3).** To a solution of *cis*-[$PtCl_2$(cod)] (0.100 g, 0.267 mmol) in CH_2Cl_2 (10 mL) was added a solution of $PASO_2$ (0.111 g, 0.536 mmol) in CH_2Cl_2 (20 mL). After ca. 15 min the colorless precipitate was isolated by filtration, washed with Et_2O, and dried in air. Yield: 0.159 g (87%). ^{31}P{^{1}H} NMR (162 MHz, dmso-d_6): δ −64.0 J_{Pt-P} = 3387 Hz. ^{1}H NMR (400 MHz, dmso-d_6): δ 4.47 (s, 4 H, PCH_2NS), 4.92 (AB quart., J = 15.6 Hz, 8 H, PCH_2N), 4.99 (AB quart., J = 13.2 Hz, 8 H, NCH_2N). Anal. Calcd for $C_{10}H_{20}N_6O_4P_2S_2Cl_2Pt$: C, 17.65; H, 2.96; N, 12.35. Found: C, 17.58; H, 3.00; N, 12.21.

[Pt(N$_3$)$_2$(PASO$_2$)$_2$] (4). To a solution of *cis*-[$Pt(N_3)_2$(cod)] (0.050 g, 0.129 mmol) in CH_2Cl_2 (5 mL) was added a solution of $PASO_2$ (0.055 g, 0.265 mmol) in CH_2Cl_2 (10 mL). After ca. 1 h the colorless precipitate was isolated by filtration, washed with MeOH, and dried in air. Yield: 0.077 g (85%). ^{31}P{^{1}H} NMR (162 MHz, dmso-d_6): δ −68.9 J_{Pt-P} = 3257 Hz. ^{1}H NMR (400 MHz, dmso-d_6): δ 4.36 (s, 4 H, PCH_2NS), 4.73−5.21 (m, 16 H, PCH_2N, NCH_2N). IR (KBr disk): 2064 $\nu(N_3)$ cm^{-1}. Anal. Calcd for $C_{10}H_{20}N_{12}O_4P_2S_2Pt$: C, 17.32; H, 2.91; N, 24.24. Found: C, 17.44; H, 2.83; N, 24.07.

[Ru(η^6-*p*-cym)Cl$_2$(PASO$_2$)] (5). To a solution of [$Ru(\eta^6$-*p*-cym)$Cl_2]_2$ (0.153 g, mmol) in MeOH (10 mL) was added a solution of $PASO_2$ (0.079 g, 0. mmol) in $MeOH_2$ (20 mL). After refluxing the mixture for ca. 4 h the orange solid was isolated by filtration, washed with MeOH, and dried in air. Yield: 0.165 g (98%). ^{31}P{^{1}H} NMR (162 MHz, dmso-d_6): δ −45.5. ^{1}H NMR (400 MHz, dmso-d_6): δ 1.11 (d, J = 6.9 Hz, 6 H, Me), 1.91 (s, 3 H, Me), 2.56 (sept, J = 6.9 Hz, 1 H, Me_2CH), 4.29 (s, 2 H, PCH_2NS), 4.66 (AB quart., J = 16.7 Hz, 4 H, PCH_2N), 5.00 (AB quart., J = 13.8 Hz, 4 H, NCH_2N), 5.81 (dd, J = 6.4/0.9 Hz, 2 H, *p*-cym), 5.86 (dd, J = 6.3/1.0 Hz, 2 H, *p*-cym). Anal. Calcd for $C_{15}H_{24}N_3O_2PSCl_2Ru$: C, 35.09; H, 4.71; N, 8.18. Found: C, 34.95; H, 5.01; N, 7.92. X-ray quality crystals were obtained by slow diffusion of EtOH into a dmso solution of the compound.

[Rh(η^5-C$_5$Me$_5$)Cl$_2$(PASO$_2$)] (6). To a solution of [$Rh(\eta^5$-$C_5Me_5)Cl_2]_2$ (0.030 g, 0.049 mmol) in MeOH (20 mL) was added $PASO_2$ (0.021 g, 0.101 mol). The solution was heated to reflux for ca. 1 h. Upon cooling, a red-orange precipitate formed, which was isolated by filtration, washed with MeOH, and subsequently dried in air. Yield: 0.055 g (82%). ^{31}P{^{1}H} NMR (162 MHz, dmso-d_6): δ −45.8 (d, J_{Rh-P} = 148 Hz). ^{1}H NMR (400 MHz, dmso-d_6): δ 1.64 (d, J = 3.9 Hz, 15 H, Me), 4.20 (s, 2 H, PCH_2NS), 4.70 (AB quart., J = 16.4 Hz, 4 H, PCH_2N), 4.99

(34) Usón, R.; Laguna, A.; Laguna, M. *Inorg. Synth.* **1989**, *26*, 85.
(35) Clark, H. C.; Manzer, L. E. *J. Organomet. Chem.* **1973**, *59*, 411.
(36) Kim, Y. J.; Choi, J. C.; Park, K. H. *Bull. Korean Chem. Soc.* **1994**, *15*, 690.
(37) Bennett, M. A.; Smith, A. K. *J. Chem. Soc., Dalton Trans.* **1974**, 233.
(38) El Amouri, H.; Gruselle, M.; Jaouén, G. *Synth. React. Inorg. Met. Org. Chem.* **1994**, *24*, 395.
(39) Boehm, A.; Schreiner, B.; Steiner, N.; Urban, R.; Suenkel, K.; Polborn, K.; Beck, W. *Z. Naturforsch. B* **1998**, *53*, 191.
(40) Komatsu, T.; Nonoyama, M. *J. Inorg. Nucl. Chem.* **1977**, *39*, 1161.

Table 4. Crystallographic and Refinement Details of Compounds 5−9

	5	6	7a	8	9
empirical formula	$C_{15}H_{24}O_2N_3PRuSCl_2$	$C_{15}H_{25}O_2N_3PRhSCl_2$	$C_{20}H_{38}O_5N_6P_2RhS_2Cl_2$	$C_{22}H_{26}O_4N_4PPdSCl$	$C_{17.25}H_{23}N_4O_2PPdCl_2S$
color	orange	orange	orange	colorless	pale yellow
M_r, g mol^{-1}	513.38	516.22	741.43	615.35	558.73
cryst syst	monoclinic	monoclinic	monoclinic	monoclinic	monoclinic
space group	$C2/c$	$P2_1/c$	$P2_1/n$	$P2_1/c$	$P2_1/n$
a, Å	28.692(2)	10.3140(3)	9.6662(3)	14.2326(6)	10.1513(3)
b, Å	6.6083(3)	7.2646(2)	12.8410(3)	16.3432(8)	18.4785(4)
c, Å	23.5466(18)	25.8648(9)	22.4541(6)	10.3295(4)	12.2060(4)
β, deg	119.812(10)	91.221(3)	92.357(3)	100.316(4)	111.010(3)
V, Å^3	3873.8(4)	1937.53(10)	2784.70(12)	2363.85(18)	2137.41(10)
Z	8	4	4	4	4
D_{calc}, g cm^{-3}	1.761	1.770	1.768	1.729	1.736
μ, mm^{-1}	1.291	1.363	1.115	1.093	1.313
$F000$	2080	1048	1520	1248	1126
θ range	3.15 to 29.48°	2.91 to 29.40°	3.15 to 29.53°	2.89 to 29.49°	3.08 to 29.45°
reflns collected	9192	10 661	13 710	150 402	9779
indep reflns	4539	4531	6494	5656	5002
parameters	232	231	348	308	273
goodness-of-fit	0.825	0.989	0.905	0.852	1.086
R_1 [$I > 2\sigma(I)$]	0.0373	0.0249	0.0282	0.0377	0.0396
wR_2 (all data)	0.0639	0.0576	0.0611	0.0691	0.0522
largest diff peak/hole, e Å^{-3}	0.863/−0.688	0.422/−0.535	0.527/−0.473	0.764/−0.758	2.164/−1.742

(AB quart., J = 13.5 Hz, 4 H, NCH_2N). Anal. Calcd for $C_{15}H_{25}N_3O_2PSCl_2Rh$: C, 34.90; H, 4.88; N, 8.14. Found: C, 35.03; H, 4.97; N, 8.36.

[Rh(η^5-C_5Me_5)Cl($PASO_2$)$_2$]BPh_4 (7). To a solution of [Rh(η^5-C_5Me_5)Cl_2]$_2$ (0.030 g, 0.049 mmol) in MeOH (20 mL) was added $PASO_2$ (0.042 g, 0.203 mol). The solution was heated to reflux for ca. 1 h, and then Na[BPh_4] (0.037 g, excess) was added. After cooling to rt, the solvent was removed under vacuum and the yellow residue was extracted with CH_2Cl_2. The solution was passed through Celite, and addition of Et_2O precipitated a yellow solid. This was isolated by filtration, washed with H_2O and Et_2O, and subsequently dried in air. Yield: 0.078 g (80%). $^{31}P\{^1H\}$ NMR (162 MHz, acetone-d_6): δ −50.9 (d, J_{Rh-P} = 136 Hz). ^1H NMR (400 MHz, acetone-d_6): δ 2.81 (s, 15 H, Me), 4.56 (s, 5 H, PCH_2NS), 4.83−5.09 (m, 16 H, PCH_2N, NCH_2N), 6.77 (t, J = 7.2 Hz, 4 H, p-BPh_4), 6.92 (t, J = 7.4 Hz, 8 H, m-BPh_4), 7.34 (m, 8 H, o-BPh_4). Anal. Calcd for $C_{44}H_{55}N_6O_4P_2S_2ClBRh$: C, 52.47; H, 5.50; N, 8.34. Found: C, 52.63; H, 5.53; N, 8.53. Positive ion HR-ES-MS (m/z): 687.0375 $[M]^+$, 480.0140 $[M - PASO_2]^+$. X-ray quality crystals of the chloride salt (**7a**) were obtained by combining small quantities of [Rh(η^5-C_5Me_5)Cl_2]$_2$ and $PASO_2$ in a vial with CH_2Cl_2 and shaking with H_2O (in an attempt to extract any water-soluble complex). Orange needles were formed after standing for 48 h.

[PdCl{κC,N-C_6H_4C(Ph)NCH_2CO_2Et}($PASO_2$)] (8). To a solution of [PdCl{κC,N-C_6H_4C(Ph)NCH_2CO_2Et}]$_2$ (0.050 g, 0.061 mmol) in CH_2Cl_2 (10 mL) was added $PASO_2$ (0.025 g, 0.120 mmol), and the mixture was stirred at rt for ca. 1 h. The solution was passed through Celite and concentrated under vacuum. Careful addition of hexane afforded fine, pale yellow needles after standing for several hours. These were isolated by filtration and dried in air. Yield: 0.056 g (75%). $^{31}P\{^1H\}$ NMR (162 MHz, dmso-d_6): δ −57.1. ^1H NMR (400 MHz, dmso-d_6): δ 1.12 (t, J = 7.1 Hz, 3 H, Me), 4.05 (q, J = 7.1 Hz, 2 H, OCH_2), 4.48 (s, 2 H, NCH_2), 4.52 (s, 2 H, PCH_2NS), 5.00 (AB quart., J = 16.2 Hz, 4 H, PCH_2N), 5.07 (AB quart., J = 13.8 Hz, 4 H, NCH_2N), 6.62 (dd, J = 7.6/1.5 Hz, 1 H, H^6), 7.08 (dt, J = 7.7/0.7 Hz, 1 H, H^5), 7.25 (dt, J = 7.5/1.5 Hz, 1 H, H^4), 7.27−7.30 (m, 2 H, o-Ph), 7.35 (d, J = 7.6 Hz, 1 H, H^3), 7.57−7.61 (m, 3 H, m-Ph, p-Ph). Anal. Calcd for $C_{22}H_{26}N_4O_4PSClPd$: C, 42.94; H, 4.26; N, 9.10. Found: C, 43.17; H, 4.11; N, 9.38. X-ray quality crystals were selected from the bulk sample.

[PdCl(κC,N-1,8-$C_{10}H_6NMe_2$)($PASO_2$)] (9). This was prepared as described above from [PdCl{κC,N-1,8-$C_{10}H_6NMe_2$}]$_2$ (0.100 g, 0.160 mmol) and $PASO_2$ (0.067 g, 0.323 mmol) to give 0.110 g (66%) of a pale yellow solid. $^{31}P\{^1H\}$ NMR (162 MHz, $CDCl_3$): δ −56.2. ^1H NMR (400 MHz, $CDCl_3$): δ 3.36 (2 s, 3 H each, NMe), 4.59 (s, 2 H, PCH_2NS), 5.01 (AB quart., J = 16.0 Hz, 4 H, PCH_2N), 5.02 (AB quart., J = 13.7 Hz, 4 H, NCH_2N), 7.34 (t, J = 7.0 Hz, 1 H, Arom), 7.38 (t, J = 7.6 Hz, 1 H, Arom), 7.45−7.51 (m, 2 H, Arom), 7.65 (d, J = 8.0 Hz, 1 H, Arom), 7.72 (dd, J = 7.2/1.6 Hz, 1 H, Arom). Anal. Calcd for $C_{22}H_{26}N_4O_4PSClPd \cdot 1/2CH_2Cl_2$: C, 37.42; H, 4.13; N, 9.97. Found: C, 37.60; H, 4.33; N, 10.15. X-ray quality crystals were selected from the bulk sample.

X-ray Diffraction Studies. Diffraction data were collected at 150 K using an Oxford Diffraction Gemini E Ultra diffractometer, equipped with an EOS CCD area detector and a four-circle kappa goniometer. For the data collection the Mo source emitting graphite-monochromated Mo Kα radiation (λ = 0.71073 Å) was used. Data integration, scaling, and empirical absorption correction were carried out using the CrysAlis Pro program package.[41] The structure was solved using direct methods and refined by full-matrix-least-squares against F^2. The non-hydrogen atoms were refined anisotropically, and hydrogen atoms were placed at idealized positions and refined using the riding model. All calculations were carried out using the program Olex2.[42] Important crystallographic data and refinement details are summarized in Table 4. The ^{i}Pr group of the p-cymene ring in complex **5** was disordered over two positions caused by rotation about the CH−Ar axis. The disordered group was refined isotropically. Complex **7a** crystallized with one molecule of water in the unit cell, the hydrogen atoms of which were not located. The unit cell of complex **9** contained half a molecule of CH_2Cl_2, the carbon atom of which was located on an inversion center disordered over two positions. The occupancy factors of the chlorine atoms were refined; the carbon atom was split over the two positions with 25% occupancy each, and the C−Cl distances were fixed at 1.74 Å. No hydrogen atoms were added to the disordered CH_2Cl_2 molecule. The highest remaining electron density peaks are located close to the Cl atoms of the disordered solvent.

Computational Studies. Full geometry optimization of PTA and $PASO_2$ ligands was done using the B3LYP/6-31G(d,p) level

(41) *CrysAlis Pro 171.33.42*; Oxford Diffraction Ltd., 2009.
(42) Dolomanov, O. V.; Bourhis, L. J.; Gildea, R. J.; Howard, J. A. K.; Puschmann, H. *J. Appl. Crystallogr.* **2009**, *42*, 339.

of density functional theory (DFT). Further, the hybrid QM-MM level optimization of the ligands was done using the ONIOM-(B3LYP/6-31G(d,p):UFF) method. At both DFT and QM-MM levels, the molecular electrostatic potential (MESP) of the ligands was calculated. The most negative-valued point of the MESP (designated as V_{min}) at the lone pair region of the phosphorus atom was determined at both levels of calculation. All the calculations were done using the Gaussian03 suite of programs.[26]

Acknowledgment. We thank the DFG for a grant to purchase the diffractometer as well as the University of Wuppertal for funding.

Supporting Information Available: Full crystallographic details of compounds **5**−**9** in CIF format as well as further details on the computational studies are available free of charge via the Internet at http://pubs.acs.org.